Hindawi Publishing Corporation
Advances in High Energy Physics
Volume 2014, Article ID 569079, 9 pages
http://dx.doi.org/10.1155/2014/569079

*Research Article*

# Pseudorapidity Distribution of Charged Particles and Square Speed of Sound Parameter in $p$-$p$ or $p$-$\overline{p}$ Collisions over an Energy Range from 0.053 to 7 TeV

**Ya-Qin Gao, Tian Tian, Li-Na Gao, and Fu-Hu Liu**

*Institute of Theoretical Physics, Shanxi University, Taiyuan, Shanxi 030006, China*

Correspondence should be addressed to Fu-Hu Liu; fuhuliu@163.com

Received 20 February 2014; Accepted 28 March 2014; Published 22 April 2014

Academic Editor: George Siopsis



Pseudorapidity distributions of charged particles produced in proton-proton ($p$-$p$) or proton-antiproton ($p$-$\overline{p}$) collisions over an energy range from 0.053 to 7 TeV are studied by using the four-component Landau hydrodynamic model. The results calculated by the model are in agreement with the experimental data of the UA5, PHOBOS, UA1, P238, CDF, ALICE, and CMS Collaborations which present orderly from low to high energies. According to the distribution widths of different components, the values and some features of square speed of sound parameter $c_s^2$ for "participant" and "spectator" quark components are obtained. It is shown that the speed of sound for "participant" quark components agrees approximately with that for "spectator" quark components in the error ranges. The present work is useful for studying nucleus-nucleus collisions in the related energy range.

## 1. Introduction

In the laboratory conditions, the only way for creating and studying the interacting systems with hadronic or partonic degrees of freedom at extremely high energy and density is to investigate heavy-ion (nucleus-nucleus) collisions at very high center-of-mass energies. The relativistic heavy ion collider (RHIC) in the United States and the large hadron collider (LHC) in Switzerland have been built, respectively [1, 2]. Particularly, the LHC was originally designed to accelerate two protons up to total energy of 14 TeV, and it will accelerate heavy ions to collide at center-of-mass energy ($\sqrt{s_{NN}}$) of 5.5 TeV. Such high energy collisions offer a new environment which leads to a new significant extension of the kinematic range in longitudinal rapidity and transverse momentum [3]. It also provides a new chance for us to understand systematically the particle statistical behavior, production process, interaction mechanism, and correlation phenomena.

The multiplicity and (pseudo)rapidity distributions of final-state particles can often be used to test different theoretical models and wonderful ideas. The rapidity distribution $dN_{ch}/dy$ and the pseudorapidity distribution $dN_{ch}/d\eta$ of charged particles are very important quantities for the study of mainly particle production mechanism in high energy nucleon-nucleon and nucleus-nucleus collisions. The studies of $dN_{ch}/dy$ and $dN_{ch}/d\eta$ in proton-proton ($p$-$p$) or proton-antiproton ($p$-$\overline{p}$) collisions not only can provide reference and baseline for heavy-ion collisions, but also can reflect the main particles contribution to heavy-ion collisions. In $p$-$p$ or $p$-$\overline{p}$ collisions at present colliders, the center-of-energies reach a region of ultrahigh energies. Meanwhile, the highest energy nuclear experiments can be performed. Most of high-density experimental data can help us realize the creation of a new state of matter, namely, the quark gluon plasma (QGP) [4, 5], which is a thermalized system consisting of strong coupling quarks and gluons in a very small region. It is believed that the QGP was the main matter in our early universe shortly after the Big Bang.

Many models have been introduced in the field of high energy collisions, for example, the hydrodynamics model [6], the thermodynamics model [7], the hadron resonance gas model [8], the fireball model [9, 10], and so forth. Generally

speaking, a given model treats the different collisions by different considerations, and different models approach the same collisions in different methods. In our previous work [11], based on the participant-spectator model [12] and Landau hydrodynamic model [13–17], the pseudorapidity distributions of charged particles produced in nucleus-nucleus collisions at the RHIC and LHC have been analyzed, and the values of square speed of sound ($c_s^2$) have been obtained. We notice that the related data for $p$-$p$ or $p$-$\overline{p}$ collisions are absent in our previous work [11].

To make up the limitation of our previous work [11], in this work, we will use the same method to study the pseudorapidity distributions of charged particles produced in $p$-$p$ or $p$-$\overline{p}$ collisions over an energy range from 0.053 to 7 TeV and to extract the values of speed of sound parameter for the "participant" and "spectator" quark components which correspond, respectively, to the participant and spectator nucleons in nucleus-nucleus collisions. The quoted experimental data are taken from the UA5 ($p$-$\overline{p}$ collisions at 0.053, 0.2, 0.546, and 0.9 TeV) [18], PHOBOS ($p$-$p$ collisions at 0.2 and 0.41 TeV) [19], UA1 ($p$-$\overline{p}$ collisions at 0.54 TeV) [20], P238 ($p$-$\overline{p}$ collisions at 0.63 TeV) [21], CDF ($p$-$\overline{p}$ collisions at 0.63 and 1.8 TeV) [22], ALICE ($p$-$p$ collisions at 0.9 and 2.36 TeV) [23], and CMS ($p$-$p$ collisions at 0.9, 2.36, and 7 TeV) [24, 25] Collaborations.

## 2. The Model

The picture of participant-spectator model [12] is the base of many theoretical models such as the nuclear fireball model [26], the two-component model [27], the nuclear overlap model [28], and the multisource thermal model [29, 30]. In the framework of participant-spectator model [12], the projectile and target nuclei penetrating through each other in collisions. Then, a central participant region, a target spectator region, and a projectile spectator region are expected to form in the collisions. Further, we can divide the participant region into two parts: a target participant region and a projectile participant region. In the multisource thermal model [29, 30], these regions can extend to different cylinders in rapidity space. In addition, the contributions of leading nucleons can fall under the spectator regions. In high energy nucleus-nucleus collisions, both the participant and spectator regions consist of nucleons.

In high energy hadron-hadron collisions, the situation is different. If we use the picture of participant-spectator model [12], both the participant and spectator regions will be quarks. Similarly, we have four source components: the target spectator quark component, the target participant quark component, the projectile participant quark component, and the projectile spectator quark component, which are presented orderly from low to high in the rapidity space. According to [31, 32], if we use the Landau hydrodynamic model [13–17] to describe the hadron-hadron collisions, only the central pseudorapidity region can be fitted. This means that the Landau hydrodynamic model [13–17] gives a narrow pseudorapidity distribution, and the contributions of leading nucleons are not included in the model. To describe the pseudorapidity distribution in a wide region, we can apply the model for each quark component in the hadron-hadron collisions.

The pseudorapidity distribution of charged particles produced in each quark component is given by a Gaussian function [17, 33]

$$\frac{dN_{\rm ch}}{d\eta} = \frac{K\left(\sqrt{s_{NN}}\right)^{1/2}}{\sqrt{2\pi\sigma_\eta^2}} \exp\left(-\frac{\eta^2}{2\sigma_\eta^2}\right) \tag{1}$$

with

$$\sigma_\eta = \sqrt{\frac{8}{3}\frac{c_s^2}{1-c_s^4}\ln\left(\frac{\sqrt{s_{NN}}}{2m_p}\right)}, \tag{2}$$

where $K$ is the normalization constant, $\sqrt{s_{NN}}$ is in the units of GeV, $c_s$ denotes the speed of sound, $m_p$ denotes the proton mass in the units of GeV/$c^2$ with $c = 1$, and $\sigma_\eta$ is the pseudorapidity distribution width.

Strictly speaking, there are some differences between the rapidity distribution and the pseudorapidity distribution. In fact, the differences between the two distributions at high energies can be neglected due to the small values [34]. If we need to distinguish the two distributions, we should calculate them severally or make a complete transformation [35]. In the present work, we do not distinguish the two distributions for the purpose of simpleness. Equation (1) can be rewritten as the function of $c_s^2$

$$\frac{dN_{\rm ch}}{d\eta} = K\left(\sqrt{s_{NN}}\right)^{1/2}\left[\frac{16\pi}{3}\frac{c_s^2}{1-c_s^4}\ln\left(\frac{\sqrt{s_{NN}}}{2m_p}\right)\right]^{-1/2} \cdot \exp\left\{-\eta^2\left[\frac{16}{3}\frac{c_s^2}{1-c_s^4}\ln\left(\frac{\sqrt{s_{NN}}}{2m_p}\right)\right]^{-1}\right\} \tag{3}$$

due to (2). The final-state pseudorapidity distribution is a weighted sum of four equations (3) with different rapidity shifts and weights.

For $p$-$p$ or $p$-$\overline{p}$ collisions, the rapidity shift ($y_{\rm TS}$) of target spectator is opposite to the rapidity shift ($y_{\rm PS}$) of projectile spectator, and the rapidity shift ($y_{\rm TP}$) of target participant is opposite to the rapidity shift ($y_{\rm PP}$) of projectile participant. The weight ($k$) of target participant is equal to that of projectile participant, and the weight $[(1-2k)/2]$ of target spectator is equal to that of projectile spectator.

## 3. Comparisons with Experimental Data

Figures 1(a)–1(d) show the pseudorapidity distributions of charged particles produced in inelastic $p$-$\overline{p}$ collisions at $\sqrt{s_{NN}}$ = 0.053, 0.2, 0.546, and 0.9 TeV, respectively. The symbols in the range of $\eta > 0$ represent the experimental data of the UA5 Collaboration [18], and those in the range of $\eta < 0$ are symmetrical reflection at the midpseudorapidity. The curves are our calculated results with the four-component Landau hydrodynamic model. The values of parameters obtained by fitting the experimental data are given in Table 1 with the values of $\chi^2$/dof ($\chi^2$ per degree of freedom), where $c_s^2(P)$ and

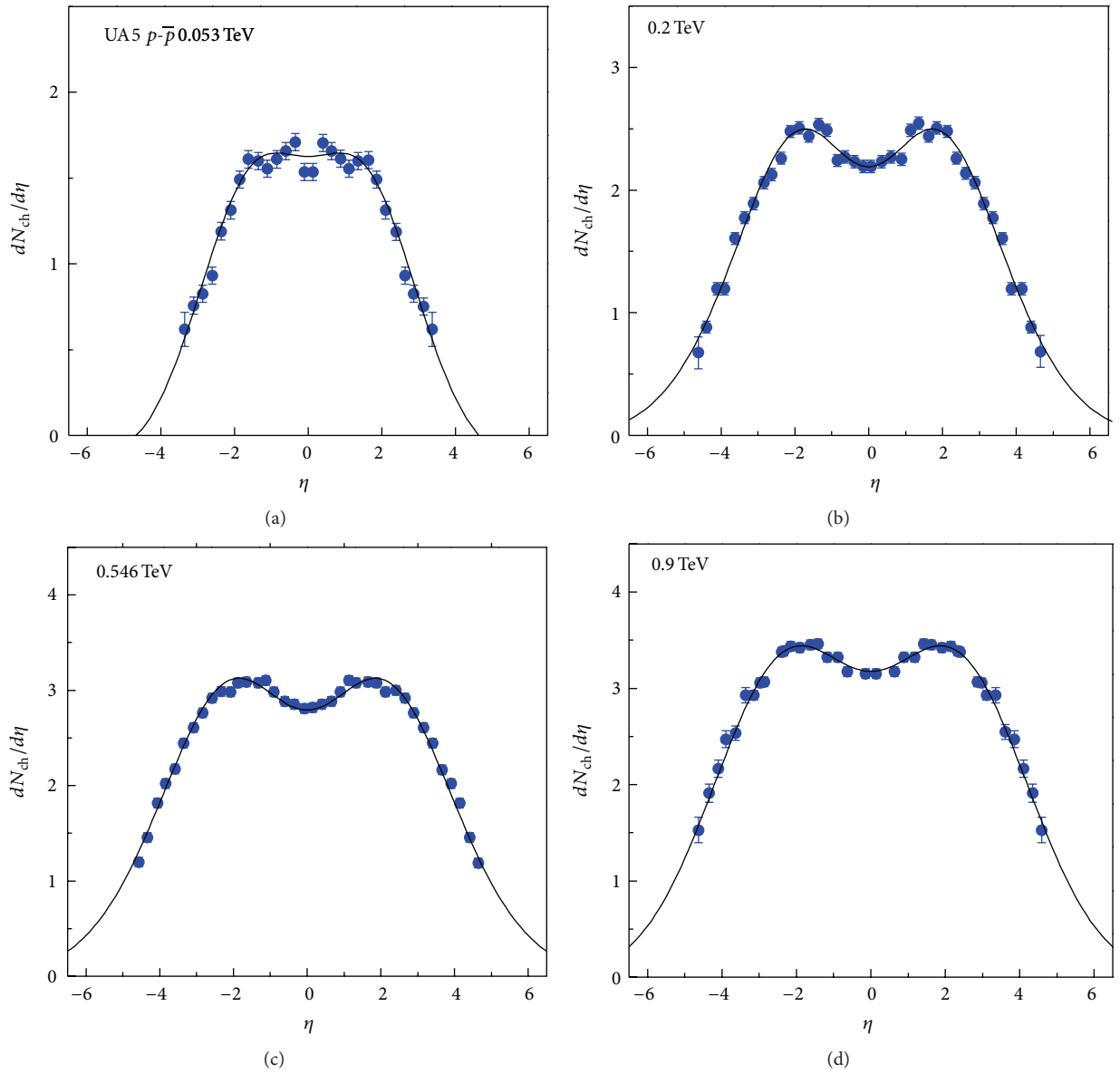


FIGURE 1: The pseudorapidity distributions, $dN_{ch}/d\eta$, of charged particles produced in inelastic $p$-$\overline{p}$ collisions at $\sqrt{s_{NN}}$ = 0.053 (a), 0.2 (b), 0.546 (c), and 0.9 TeV (d). The symbols represent the experimental data of the UA5 Collaboration [18], and the curves are our calculated results.

$c_s^2(S)$ denote the square speeds of sound for the participants and spectators, respectively. One can see that the calculated results are in agreement with the experimental data at the four energies. Both values of $c_s^2$ for the participants and spectators are approximately equal to each other in the error ranges, and they do not depend obviously on $\sqrt{s_{NN}}$ in the considered energy range.

The pseudorapidity distributions of charged particles produced in inelastic $p$-$p$ collisions at $\sqrt{s_{NN}}$ = 0.2 and 0.41 TeV measured by the PHOBOS Collaboration [19], $p$-$\overline{p}$ collisions at $\sqrt{s_{NN}}$ = 0.54 TeV measured by the UA1 Collaboration [20], $p$-$\overline{p}$ collisions at $\sqrt{s_{NN}}$ = 0.63 TeV measured by the P238 Collaboration with $|\eta|$ ranging from 1.5 to 5.5 [21], and $p$-$\overline{p}$ collisions at $\sqrt{s_{NN}}$ = 0.63 and 1.8 TeV measured by the CDF Collaboration with $|\eta|$ = 0–3.5 [22] are presented in Figures 2(a)–2(f), respectively. The symbols and curves represent the same meanings as those in Figure 1. By fitting the experimental data, the obtained values of $c_s^2$ and $\chi^2$/dof are given in Table 1. Once again the four-component Landau hydrodynamic model describes the experimental data well. Although the energy has a large change, the values of $c_s^2$ for the participants and spectators are approximately the same in the error ranges, and they have no obvious change with changing the energy.

Figure 3 gives the pseudorapidity distributions of charged particles produced in non-single-diffractive $p$-$p$ collisions at $\sqrt{s_{NN}}$ = 0.9, 2.36, and 7 TeV. The symbols in the left panel represent the experimental data obtained by the CMS

Table 1: Values of $c_s^2$, other parameters, and $\chi^2$/dof corresponding to the curves in Figures 1–3.

| Figure | Collisions | $\sqrt{s_{NN}}$ (TeV) | $c_s^2$ $(P)$ | $c_s^2$ $(S)$ | $y_{PP}$ | $y_{PS}$ | $k$ | $\chi^2$/dof |
|---|---|---|---|---|---|---|---|---|
| Figure 1(a) | $p$-$\overline{p}$ | 0.053 | 0.24 ± 0.06 | 0.24 ± 0.06 | 1.50 ± 0.08 | 3.10 ± 0.50 | 0.472 ± 0.016 | 0.062 |
| Figure 1(b) | $p$-$\overline{p}$ | 0.200 | 0.19 ± 0.02 | 0.19 ± 0.07 | 1.81 ± 0.06 | 4.00 ± 0.05 | 0.419 ± 0.012 | 0.064 |
| Figure 1(c) | $p$-$\overline{p}$ | 0.546 | 0.20 ± 0.03 | 0.20 ± 0.10 | 2.01 ± 0.07 | 4.30 ± 0.09 | 0.437 ± 0.015 | 0.038 |
| Figure 1(d) | $p$-$\overline{p}$ | 0.900 | 0.22 ± 0.04 | 0.21 ± 0.09 | 2.01 ± 0.11 | 3.50 ± 0.05 | 0.398 ± 0.015 | 0.026 |
| Figure 2(a) | $p$-$p$ | 0.200 | 0.20 ± 0.01 | 0.18 ± 0.02 | 1.81 ± 0.04 | 3.90 ± 0.20 | 0.419 ± 0.009 | 0.009 |
| Figure 2(b) | $p$-$p$ | 0.410 | 0.20 ± 0.01 | 0.21 ± 0.03 | 1.94 ± 0.03 | 3.95 ± 0.15 | 0.402 ± 0.010 | 0.009 |
| Figure 2(c) | $p$-$\overline{p}$ | 0.540 | 0.20 ± 0.05 | 0.18 ± 0.04 | 1.78 ± 0.07 | 4.00 ± 0.50 | 0.420 ± 0.020 | 0.023 |
| Figure 2(d) | $p$-$\overline{p}$ | 0.630 | 0.22 ± 0.04 | 0.21 ± 0.06 | 1.81 ± 0.19 | 3.95 ± 0.05 | 0.343 ± 0.024 | 0.017 |
| Figure 2(e) | $p$-$\overline{p}$ | 0.630 | 0.15 ± 0.03 | 0.22 ± 0.05 | 1.79 ± 0.05 | 3.95 ± 0.02 | 0.318 ± 0.011 | 0.035 |
| Figure 2(f) | $p$-$\overline{p}$ | 1.800 | 0.16 ± 0.03 | 0.24 ± 0.05 | 1.99 ± 0.07 | 4.00 ± 0.33 | 0.321 ± 0.011 | 0.009 |
| Figure 3(a) | $p$-$p$ | 0.900 | 0.21 ± 0.06 | 0.21 ± 0.05 | 2.00 ± 0.03 | 3.00 ± 0.17 | 0.417 ± 0.011 | 0.002 |
| Figure 3(b) | $p$-$p$ | 0.900 | 0.18 ± 0.03 | 0.20 ± 0.05 | 2.00 ± 0.03 | 3.50 ± 0.30 | 0.417 ± 0.008 | 0.011 |
| Figure 3(c) | $p$-$p$ | 2.360 | 0.22 ± 0.06 | 0.26 ± 0.03 | 2.00 ± 0.03 | 3.98 ± 0.09 | 0.326 ± 0.004 | 0.005 |
| Figure 3(d) | $p$-$p$ | 2.360 | 0.18 ± 0.04 | 0.24 ± 0.03 | 2.00 ± 0.04 | 4.00 ± 0.13 | 0.295 ± 0.006 | 0.024 |
| Figure 3(e) | $p$-$p$ | 7.000 | 0.18 ± 0.05 | 0.23 ± 0.02 | 2.00 ± 0.04 | 4.10 ± 0.09 | 0.321 ± 0.004 | 0.004 |

Collaboration [24, 25], and those in the right panel stand for the experimental data of the ALICE Collaboration [23]. The curves are our calculated results. The obtained values of $c_s^2$ and $\chi^2$/dof are given in Table 1. We notice that the model describes the experimental data at the LHC energies. Both values of $c_s^2$ for the participants and spectators seem to be the same in the error ranges, and they do not depend obviously on the energy.

To see clearly the dependences of $c_s^2(P)$ and $c_s^2(S)$ on $\sqrt{s_{NN}}$, the values of $c_s^2(P)$ and $c_s^2(S)$ in Table 1 are displayed in Figure 4. Different symbols represent the results extracted from different experiments as marked in the figure. The open and closed symbols represent the values of $c_s^2(P)$ and $c_s^2(S)$, respectively. One can see that both the $c_s^2(P)$ and $c_s^2(S)$ fall mainly into a range consisting of two lines: $c_s^2 = 0.12$ and $c_s^2 = 0.30$. These results are in agreement with the hadron resonance gas model which results in, respectively, $c_s^2 \approx 0.23$ and $c_s^2 \approx 0.12$ for the existing regions of hadron resonances including and excluding pions at the temperature of ~85 MeV and $c_s^2 \approx 0.14$–$0.15$ for the two existing regions at the temperature of ~190 MeV [36, 37]. The present results are also in agreement with the lattice quantum chromodynamics theory which gives $c_s^2 = 0.12$–$0.16$ and 0.31 at the temperatures of 125 and 400 MeV, respectively [38].

Both values of $c_s^2$ for the participants and spectators are approximately the same in the error ranges and they do not depend obviously on $\sqrt{s_{NN}}$ over an energy range from 0.053 to 7 TeV. From Figure 4, one can also see that $c_s^2(P)$ seems to be less than $c_s^2(S)$ at TeV energies. Because the fitted errors are large for both $c_s^2$, it is hard to determine which one is less than the other.

The correlations between $y_{PP}$ and $\ln\sqrt{s_{NN}}$ as well as $y_{PS}$ and $\ln\sqrt{s_{NN}}$ are presented in Figures 5(a) and 5(b), respectively, where $\sqrt{s_{NN}}$ is in the units of GeV. The symbols represent the values of rapidity shifts $y_{PP}$ and $y_{PS}$ which are obtained in Figures 1–3 and listed in Table 1. The lines are our fitted results which are described by

$$y_{PP} = (0.071 \pm 0.010)\ln\sqrt{s_{NN}} + (1.460 \pm 0.071) \quad (4)$$

with $\chi^2$/dof = 0.514 and

$$y_{PS} = (0.017 \pm 0.030)\ln\sqrt{s_{NN}} + (3.852 \pm 0.199) \quad (5)$$

with $\chi^2$/dof = 0.863, respectively. One can see the linear relation existing between the rapidity shifts and $\ln\sqrt{s_{NN}}$. With the increase of the logarithmic center-of-mass energy, both rapidity shifts increase slightly.

The correlation between $k$ and $\ln\sqrt{s_{NN}}$ is shown in Figure 6, where $\sqrt{s_{NN}}$ is in the units of GeV. The symbols represent the values of contribution ratio of the projectile (or target) participant quark component which are obtained in Figures 1–3 and listed in Table 1. The line is our fitted result described by

$$k = -(0.026 \pm 0.001)\ln\sqrt{s_{NN}} + (0.547 \pm 0.011) \quad (6)$$

with $\chi^2$/dof = 0.646. One can see the linear relation existing between the contribution ratio and $\ln\sqrt{s_{NN}}$. Particularly, the contribution ratio of participants decreases and that of spectators increases with the increase of the logarithmic center-of-mass energy.

## 4. Conclusions

To conclude, the pseudorapidity distributions of charged particles produced in $p$-$p$ collisions at $\sqrt{s_{NN}}$ = 0.2, 0.41, 0.9, 2.36, and 7 TeV and in $p$-$\overline{p}$ collisions at $\sqrt{s_{NN}}$ = 0.053, 0.2, 0.54, 0.546, 0.63, 0.9, and 1.8 TeV have been studied in the present work. The calculated results of the four-component Landau hydrodynamical model satisfactorily describe the experimental data of the UA5, PHOBOS, UA1, P238, CDF, ALICE,

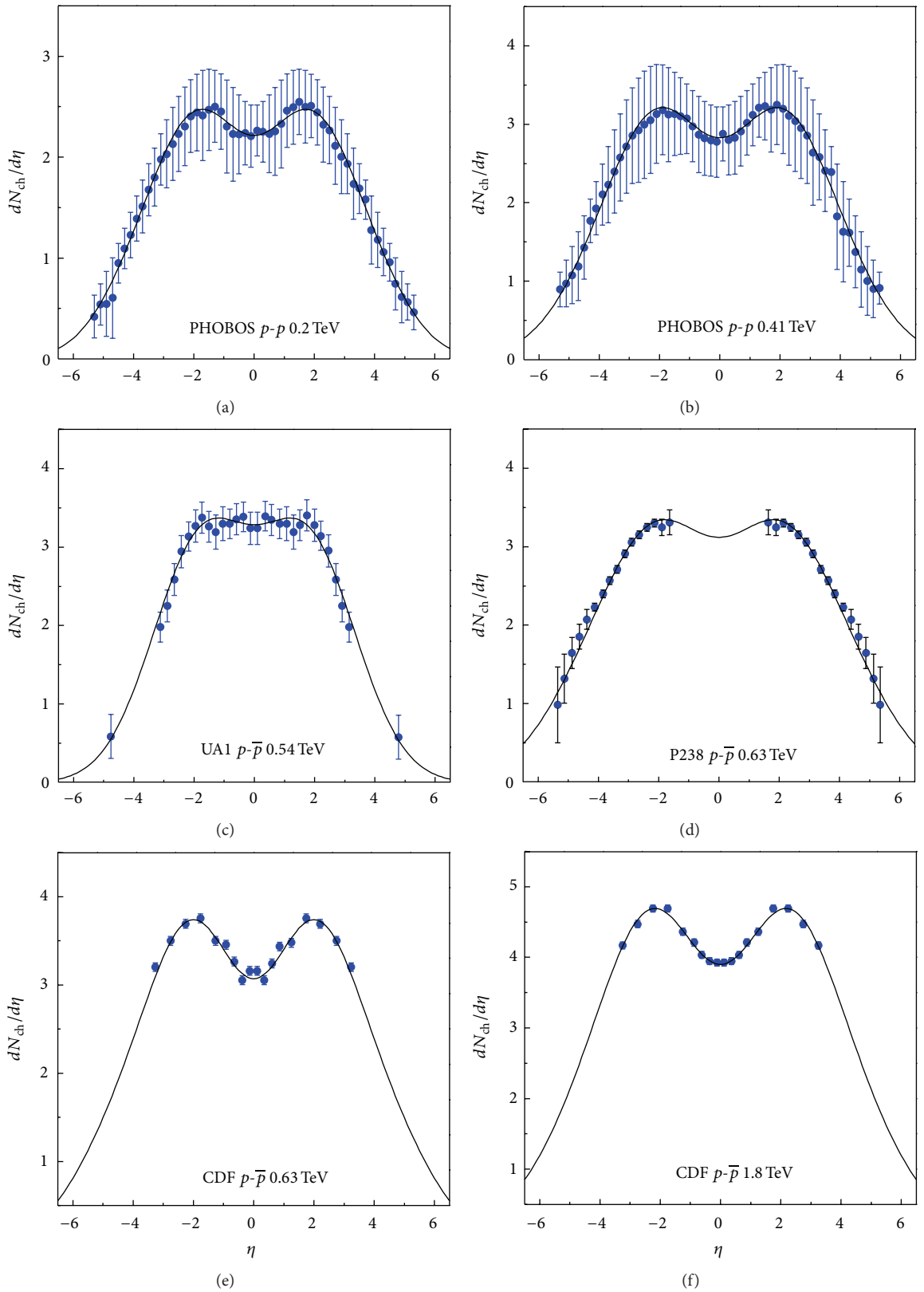


FIGURE 2: The pseudorapidity distributions of charged particles in inelastic $p$-$p$ collisions at $\sqrt{s_{NN}}$ = 0.2 (a) and 0.41 TeV (b), as well as in inelastic $p$-$\overline{p}$ collisions at $\sqrt{s_{NN}}$ = 0.54 (c), 0.63 (d, e), and 1.8 TeV (f). The symbols represent the experimental data of the PHOBOS [19] (a, b), UA1 [20] (c), P238 [21] (d), and CDF Collaborations [22] (e, f), respectively. The curves are our calculated results.

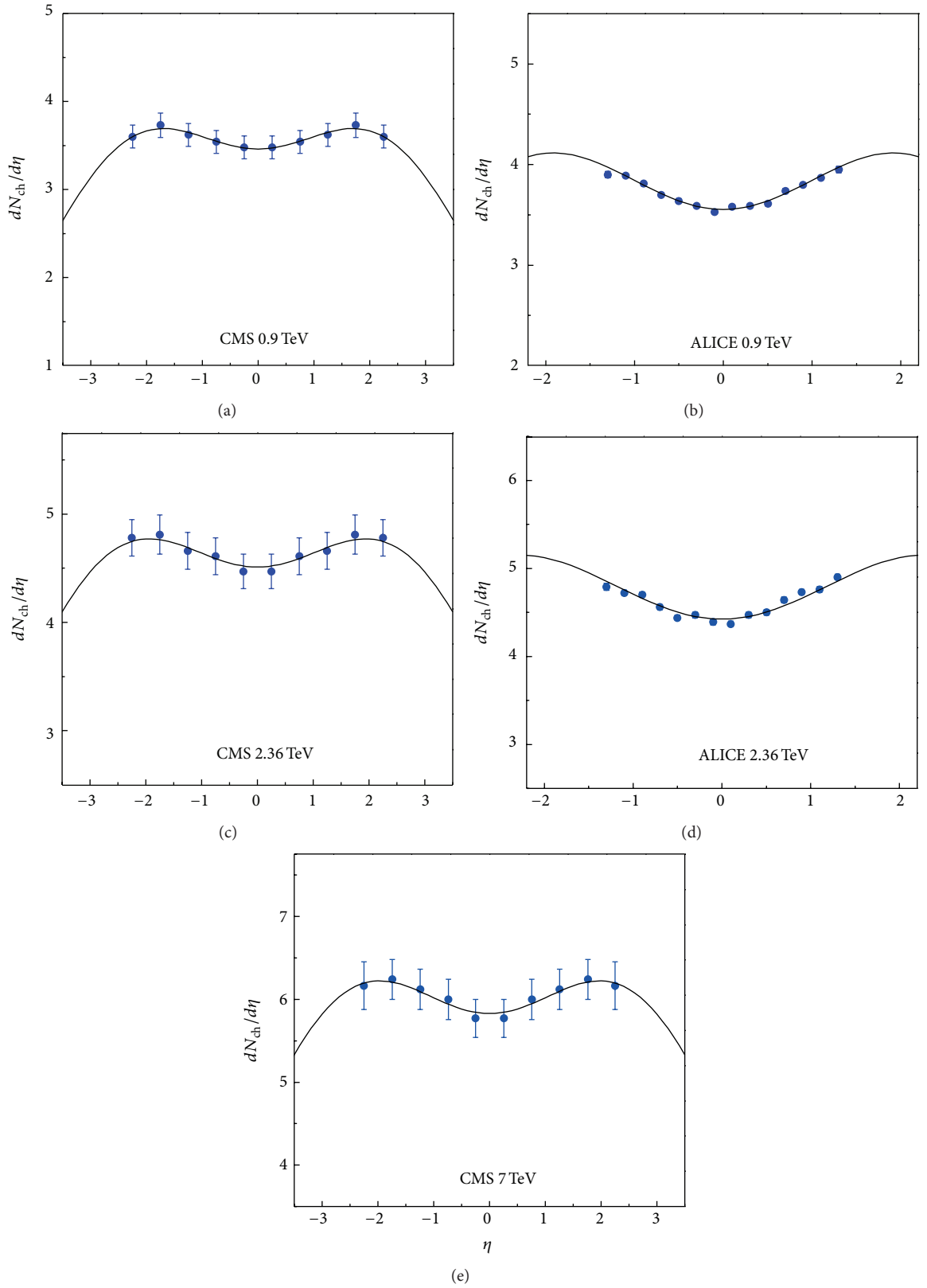


FIGURE 3: The pseudorapidity distributions of charged particles in non-single-diffractive $p$-$p$ collisions at $\sqrt{s_{NN}}$ = 0.9 (a, b), 2.36 (c, d), and 7 TeV (e). The symbols represent the experimental data of the CMS [24, 25] (a, c, e) and ALICE Collaborations [23] (b, d), and the curves are our calculated results.

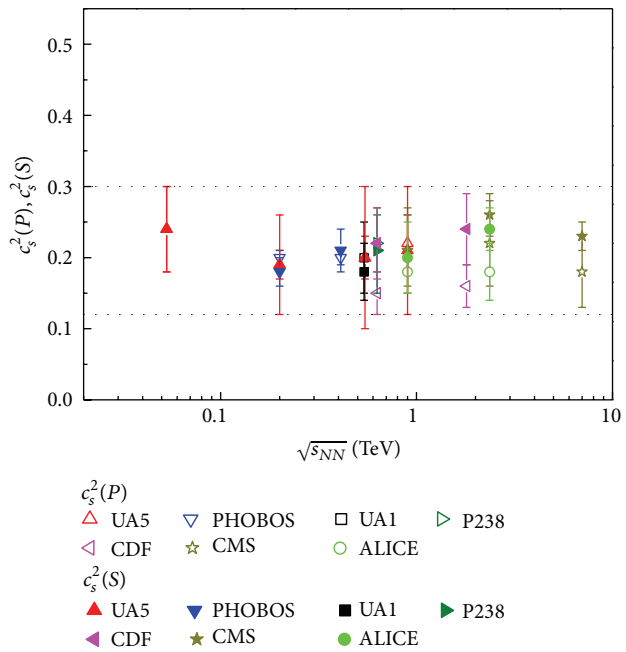


FIGURE 4: Correlations between $c_s^2$ and $\sqrt{s_{NN}}$. The closed and open symbols represent, respectively, the values of $c_s^2(P)$ and $c_s^2(S)$ obtained in Figures 1–3 and listed in Table 1. The two lines described by $c_s^2 = 0.12$ and $c_s^2 = 0.30$ show a range for different $c_s^2$.

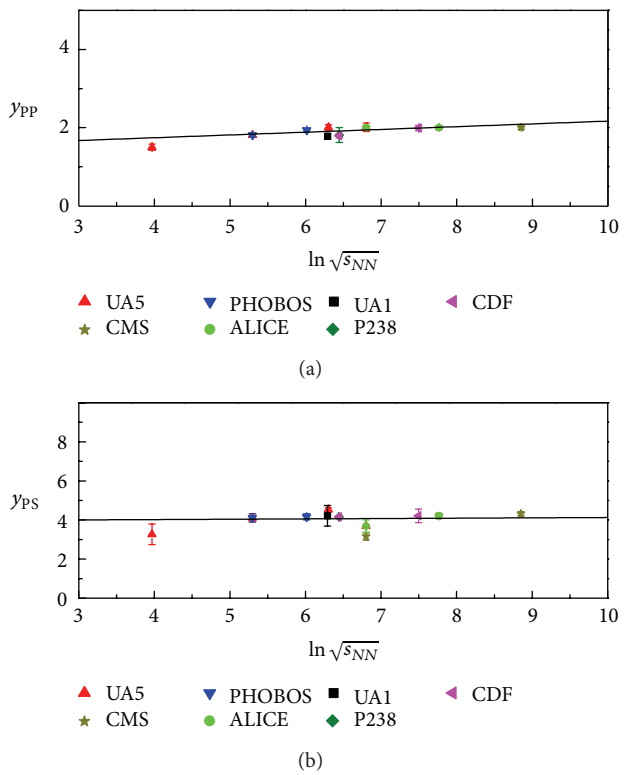


FIGURE 5: Correlations between $y_{PP}$ and $\ln \sqrt{s_{NN}}$ (a), as well as $y_{PS}$ and $\ln \sqrt{s_{NN}}$ (b), where $\sqrt{s_{NN}}$ is in the units of GeV. The symbols represent the values of rapidity shifts $y_{PP}$ and $y_{PS}$ obtained in Figures 1–3 and listed in Table 1 and the lines are our fitted results.

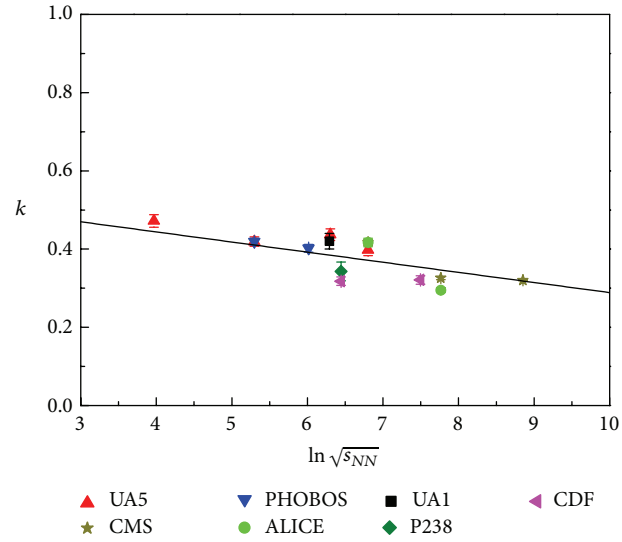


FIGURE 6: Correlations between $k$ and $\ln \sqrt{s_{NN}}$, where $\sqrt{s_{NN}}$ is in the units of GeV. The symbols represent the values of contribution ratio $k$ of projectile (or target) participant quark component obtained in Figures 1–3 and listed in Table 1, and the line is our fitted result.

and CMS Collaborations. In the model, we have considered the application of the participant-spectator model [12] in hadron-hadron collisions. Then, the interacting system of hadron-hadron collisions is divided into four components: the target and projectile "spectator" quark components and the target and projectile "participant" quark components. For each component, the Landau hydrodynamical model [13–17] is applied, which results in the pseudorapidity distribution being a Gaussian type.

Based on the above successful descriptions of the pseudorapidity distributions of charged particles produced in $p$-$p$ or $p$-$\overline{p}$ collisions over an energy range from 0.053 to 7 TeV, the square speeds of sound, $c_s^2$, for both the participants and spectators are obtained and found to be the same in the fitted error ranges. Both $c_s^2$ are approximately independent of $\sqrt{s_{NN}}$ in the considered energy range and fall mainly into the range of 0.12–0.30 which is in agreement with hadron resonance gas model which gives $c_s^2 \approx 0.12$–$0.23$ at the temperature of ~85 MeV and $c_s^2 \approx 0.14$–$0.15$ at ~190 MeV [36, 37]. The values of $c_s^2$ obtained in the present work are also in agreement with the lattice quantum chromodynamics theory which gives $c_s^2 \approx 0.12$–$0.31$ in the temperature range of 125–400 MeV [38].

In the process of extracting the speed of sound, the rapidity shifts and contribution ratio of the participant and spectator quark components are naturally obtained. There are linear relations existing between $y_{PP}$ and $\ln \sqrt{s_{NN}}$, $y_{PS}$ and $\ln \sqrt{s_{NN}}$, as well as $k$ and $\ln \sqrt{s_{NN}}$. Both rapidity shifts increase slightly with the increase of the logarithmic center-of-mass energy. The contribution ratio of participants decreases and that of the spectators increases with the increase of the logarithmic center-of-mass energy.

## 5. Discussions

The basis for Landau's equation (essentially a Gaussian pseudorapidity distribution) is the applicability of Landau hydrodynamics, namely, the creation of an initial state of dense Lorentz contracted matter that expands later according to the equations of 2 + 1 dimensional relativistic hydrodynamics. It seems that such an initial state is not created in hadron-hadron collision at intermediate or not too high energy, and the evolution of the interacting system would not be covered by hydrodynamics. However, hadron-hadron collision at high or ultrahigh energy can be regarded as a small dense system comparing with nucleus-nucleus collisions. This small dense system can produce a multihadron final-state state and can be approximately described by Landau's equation.

The square speed of sound extracted from the present work is in agreement with that from nucleus-nucleus collisions at RHIC and LHC energies in our previous work [11]. The similar values of speed of sound in both hadron-hadron and nucleus-nucleus collisions provides the insight into some common laws and universal mechanisms in multihadron productions [31, 32]. We believe that there are more similar quantities in multihadron productions in the "elementary" and "complex" collisions.

We would like to point out that the present work is the first one which extracts the square speed of sound in hadron-hadron collisions from the pseudorapidity distributions of charged particles over a very wide energy range. What we use is the four-component Landau hydrodynamic model which is based on the participant-spectator model [12] and the Landau hydrodynamic model [13–17]. Our work can provide references and baselines for nucleus-nucleus collisions at high energies. We hope to extract the square speed of sound in proton-proton and lead-lead collisions at the highest energy at the LHC in the near future.

## Conflict of Interests

The authors declare that there is no conflict of interests regarding the publication of this paper.

## Acknowledgments

This work was partly finished at the State University of New York at Stony Brook, USA. One of the authors (Fu-Hu Liu) thanks Professor Dr. Roy A. Lacey and the members of the Nuclear Chemistry Group of Stony Brook University for their hospitality. The authors acknowledge the supports of the National Natural Science Foundation of China (under Grant nos. 10975095, 11247250, and 11005071), the China National Fundamental Fund of Personnel Training (under Grant no. J1103210), the Open Research Subject of the Chinese Academy of Sciences Large-Scale Scientific Facility (under Grant no. 2060205), the Shanxi Scholarship Council of China, and the Overseas Training Project for Teachers at Shanxi University.

## References

[1] S. Chatrchyan, V. Khachatryan, A. M. Sirunyan, A. Tumasyan, W. Adam, T. Bergauer et al., "Indications of suppression of excited $\gamma$ states in Pb-Pb collisions at $\sqrt{s_{NN}} = 2.76$ TeV," *Physical Review Letters*, vol. 107, no. 23, Article ID 052302, 15 pages, 2011.

[2] A. A. Alves Jr., L. M. A. Filho, A. F. Barbosa, I. Bediaga, G. Cernicchiaro, G. Guerrer et al., "The LHCb detector at the LHC," *Journal of Instrumentation*, vol. 3, no. 8, Article ID S08005, 217 pages, 2008.

[3] R. Aaij, C. A. Beteta, A. Adametz et al. et al., "Measurement of prompt hadron production ratios in $pp$ collisions at $\sqrt{s} = 0.9$ and 7 TeV," *European Physical Journal C*, vol. 72, Article ID 2168, 19 pages, 2012.

[4] K. J. Eskola, K. Kajantie, P. V. Ruuskanen, and K. Tuominen, "Scaling of transverse energies and multiplicities with atomic number and energy in ultrarelativistic nuclear collisions," *Nuclear Physics B*, vol. 570, no. 1-2, pp. 379–389, 2000.

[5] J.-P. Blaizot, "Theoretical overview: towards understanding the quark-gluon plasma," *Journal of Physics G: Nuclear and Particle Physics*, vol. 34, no. 8, pp. S243–S251, 2007.

[6] B. M. Waldhauser, D. H. Rischke, J. A. Maruhn, H. Stöcker, and W. Greiner, "Influence of the nuclear bulk properties and the MIT bag constant on the phase transition to the quark gluon plasma," *Zeitschrift für Physik C: Particles and Fields*, vol. 43, no. 3, pp. 411–417, 1989.

[7] G. F. Bertsch and S. Das Gupta, "A guide to microscopic models for intermediate energy heavy ion collisions," *Physics Reports*, vol. 160, no. 4, pp. 189–233, 1988.

[8] F. Karsch, K. Redlich, and A. Tawfik, "Hadron resonance mass spectrum and lattice QCD thermodynamics," *The European Physical Journal C*, vol. 29, no. 4, pp. 549–556, 2003.

[9] W. Y. Zhang, "Jets induced in emulsions and cloud chambers by cosmic ray particles of energy ($10^{11} - 10^{14}$ eV)," *Acta Physica Sinica*, vol. 17, no. 8, pp. 271–295, 1961.

[10] G. D. Westfall, J. Gosset, P. J. Johansen et al., "Nuclear fireball model for proton inclusive spectra from relativistic heavy-ion collisions," *Physical Review Letters*, vol. 37, no. 18, pp. 1202–1205, 1976.

[11] L.-N. Gao, Y.-H. Chen, H.-R. Wei, and F.-H. Liu, "Speed of sound parameter from RHIC and LHC heavy-ion data," *Advances in High Energy Physics*, vol. 2013, Article ID 450247, 8 pages, 2013.

[12] R. J. Glauber, "High-energy collision theory," in *Lectures of Theoretical Physics*, W. E. Brittin and L. G. Dunham, Eds., vol. 1, pp. 315–414, Interscience, New York, NY, USA, 1959.

[13] L. D. Landau, "Multiple production of particles under collision of rapid particles," *Izvestiya Akademii Nauk: Series Fizicheskikh*, vol. 17, p. 51, 1953.

[14] L. D. Landau, "Multiple production of particles under collision of rapid particles," in *Collected Papers of L. D. Landau*, D. Ter-Haarp, Ed., pp. 569–585, Pergamon Press, Oxford, UK, 1965.

[15] "On multiple production of particles during collisions of fast particles," in *Quark-Gluon Plasma: Theoretical Foundations*, J. Kapusta, B. Mueler, and J. Rafelski, Eds., p. 283, Elsevier, Amsterdam, The Netherlands, 2003.

[16] S. Z. Belen'kji and L. D. Landau, "Hydrodynamic theory of multiple production of particles," *Il Nuovo Cimento*, vol. 3, no. 1, supplement, pp. 15–31, 1956.

[17] E. V. Shuryak, "Multiparticle production in high energy particle collisions," *Yadernaya Fizika*, vol. 16, no. 2, pp. 395–405, 1972.

[18] G. J. Alner, K. Alpgård, P. Anderer et al., "UA5: a general study of proton-antiproton physics at $\sqrt{S} = 546$ GeV," *Physics Reports*, vol. 154, no. 5-6, pp. 247–383, 1987.

[19] B. Alver, B. B. Back, M. D. Baker, M. Ballintijn, D. S. Barton, R. R. Betts et al., "Charged-particle multiplicity and pseudorapidity distributions measured with the PHOBOS detector in Au+Au, Cu+Cu, d+Au, and p+p collisions at ultrarelativistic energies," *Physical Review C*, vol. 83, no. 2, Article ID 024913, 24 pages, 2011.

[20] G. Arnison, A. Astbury, B. Aubert, C. Bacci, R. Bernabei, A. Bézaguet et al., "Charged particle multiplicity distributions in proton-antiproton collisions at 540 GeV centre of mass energy," *Physics Letters B*, vol. 123, no. 1-2, pp. 108–124, 1983.

[21] R. Harr, C. Liapis, P. Karchin et al., "Pseudorapidity distribution of charged particles in $pp$ collisions at $\sqrt{s} = 630$ GeV," *Physics Letters B: Nuclear, Elementary Particle and High-Energy Physics*, vol. 401, no. 1-2, pp. 176–180, 1997.

[22] F. Abe, D. Amidei, G. Apollinari, G. Ascoli, M. Atac, P. Auchincloss et al., "Pseudorapidity distributions of charged particles produced in $\overline{p}p$ interactions at $\sqrt{s} = 630$ and 1800 GeV," *Physical Review D*, vol. 41, no. 7, pp. 2330–2333, 1990.

[23] K. Aamodt, N. Abel, U. Abeysekara, A. A. Quintana, A. Abramyan, D. Adamová et al., "Charged-particle multiplicity measurement in proton–proton collisions at $\sqrt{s} = 0.9$ and 2.36 TeV with ALICE at LHC," *The European Physical Journal C*, vol. 68, no. 1-2, pp. 89–108, 2010.

[24] V. Khachatryan, A. M. Sirunyan, A. Tumasyan, W. Adam, T. Bergauer, M. Dragicevic et al., "Transverse momentum and pseudorapidity distributions of charged hadrons in $pp$ collisions at $\sqrt{s} = 0.9$ and 2.36 TeV," *Journal of High Energy Physics*, no. 2, Article ID 41, 35 pages, 2010.

[25] V. Khachatryan, A. M. Sirunyan, A. Tumasyan, W. Adam, T. Bergauer, M. Dragicevic et al., "Transverse-momentum and pseudorapidity distributions of charged hadrons in $pp$ collisions at $\sqrt{s} = 7$ TeV," *Physical Review Letters*, vol. 105, no. 2, Article ID 022002, 14 pages, 2010.

[26] J. Gosset, H. H. Gutbrod, W. G. Meyer et al., "Central collisions of relativistic heavy ions," *Physical Review C*, vol. 16, no. 2, pp. 629–657, 1977.

[27] L. Grandchamp and R. Rapp, "Charmonium suppression and regeneration from SPS to RHIC," *Nuclear Physics A*, vol. 709, no. 1–4, pp. 415–439, 2002.

[28] S. Eremin and S. Voloshin, "Nucleon participants or quark participants?" *Physical Review D*, vol. 67, no. 6, Article ID 064905, 3 pages, 2003.

[29] F.-H. Liu, N. N. A. Allah, and B. K. Singh, "Dependence of black fragment azimuthal and projected angular distributions on polar angle in silicon-emulsion collisions at 4.5$A$ GeV/c," *Physical Review C*, vol. 69, no. 5, Article ID 057601, 4 pages, 2004.

[30] F.-H. Liu and J.-S. Li, "Isotopic production cross section of fragments in $^{56}$Fe+p and $^{136}$Xe($^{124}$Xe)+Pb reactions over an energy range from 300$A$ to 1500$A$ MeV," *Physical Review C*, vol. 78, no. 4, Article ID 044602, 13 pages, 2008.

[31] E. K. G. Sarkisyan and A. S. Sakharov, "Relating multihadron production in hadronic and nuclear collisions," *The European Physical Journal C*, vol. 70, no. 3, pp. 533–541, 2010.

[32] E. K. G. Sarkisyan and A. S. Sakharov, "Multihadron production features in different reactions," in *Proceedings of the 35th International Symposium on Multiparticle Dynamics and the Workshop on Particle Correlations and Femtoscopy*, vol. 828 of *AIP Conference Proceedings*, pp. 35–41, Kroměříž, Czech Republic, August 2005.

[33] C. Alt, T. Anticic, B. Baatar et al. et al., "Energy dependence of particle ratio fluctuations in central Pb+Pb collisions from $\sqrt{s_{NN}} = 6.3$ to 17. 3 GeV," *Physical Review C*, vol. 79, no. 4, Article ID 044910, 11 pages, 2009.

[34] G. Wolschin, "Pseudorapidity distributions of produced charged hadrons in $pp$ collisions at RHIC and LHC energies," *Europhysics Letters*, vol. 95, no. 6, Article ID 61001, 6 pages, 2011.

[35] C. Y. Wong, *Introduction to High-Energy Heavy-Ion Collisions*, World Scientific, Singapore, 1994.

[36] A. Tawfik and H. Magdy, "Hadronic equation of state and speed of sound in thermal and dense medium," http://arxiv.org/abs/1206.0901.

[37] A. Tawfik and T. Harko, "Quark-hadron phase transitions in the viscous early universe," *Physical Review D*, vol. 85, no. 8, Article ID 084032, 19 pages, 2012.

[38] Sz. Borsányi, G. Endrődi, Z. Fodor et al., "QCD equation of state at nonzero chemical potential: continuum results with physical quark masses at order $\mu_2$," *Journal of High Energy Physics*, vol. 2012, no. 8, Article ID 53, 14 pages, 2012.